CASE REPORT

A patient with Huntington's disease and long-surviving fetal neural transplants that developed mass lesions

C. Dirk Keene · Rubens C. Chang · James B. Leverenz ·
Oleg Kopyov · Susan Perlman · Robert F. Hevner ·
Donald E. Born · Thomas D. Bird · Thomas J. Montine

Abstract Transplantation of human fetal neural tissue into adult neostriatum is an experimental therapy for Huntington's disease (HD). Here we describe a patient with HD who received ten intrastriatal human fetal neural transplants and, at one site, an autologous sural nerve co-graft. Although initially clinically stable, she developed worsening asymmetric upper motor neuron symptoms in addition to progression of HD, and ultimately died 121 months post transplantation. Eight neural transplants, up to 2.9 cm, and three ependymal cysts, up to 2.0 cm, were identified. The autologous sural nerve co-graft was found adjacent to the largest mass lesion, which, along with the ependymal cyst, exhibited pronounced mass effect on the internal capsules bilaterally. Grafts were composed of neurons and glia embedded in disorganized neuropil; robust Y chromosome labeling was present in a subset of grafts and cysts. The graft–host border was discrete, and there was no evidence of graft rejection or HD pathologic changes within donor neurons. This report, for the first time, highlights the potential for graft overgrowth in a patient receiving fetal neural transplantation.

Keywords Huntington's disease · Human fetal neural transplantation · Graft survival and differentiation · Transplant overgrowth · Peripheral nerve co-graft

C. D. Keene (✉) · R. C. Chang · R. F. Hevner · D. E. Born ·
T. J. Montine
Division of Neuropathology,
Department of Pathology, Harborview Medical Center,
University of Washington Medical Center,
Box 359791, Seattle, WA 98104, USA
e-mail: cdkeene@u.washington.edu

J. B. Leverenz · T. D. Bird
Department of Neurology,
VA-Puget Sound Health Care System,
University of Washington Medical Center,
Seattle, WA 98104, USA

R. F. Hevner
Department of Neurosurgery,
University of Washington Medical Center,
Seattle Children's Hospital and Regional Medical Center,
Seattle, WA 98104, USA

O. Kopyov
Neurosciences Institute,
St. John's Regional Medical Center,
Oxnard, CA 93030, USA

S. Perlman
Department of Neurology,
UCLA, Los Angeles, CA 90095, USA

Introduction

Huntington's disease (HD) is an autosomal dominant neurodegenerative disease characterized by progressive motor, cognitive, and psychiatric impairment mediated largely by selective loss of the medium spiny GABAergic projection neurons of the caudate nucleus and putamen. Neural transplantation as a method of cell replacement or neuroprotection has been widely investigated in multiple rodent and non-human primate models of HD that show robust interconnectivity between graft and host without negative outcomes, such as overgrowth of grafted tissue, cyst formation, or aberrant differentiation, and partial to complete recovery of lesion-induced deficits in multiple transplant paradigms (see [5] for review). These studies led to two case reports describing fetal neural transplantation in patients with HD [14, 23] followed by four clinical trials investigating the safety and efficacy of this procedure. The

first of these clinical trials was performed by Kopyov et al. [10, 21], followed by trials in Florida [8], France [1–3] and United Kingdom [22].

Results of autopsies of three HD patients who received neural transplants have been reported. The first was described by Freeman et al. [7], in which, at approximately 18 months post-transplantation, examination showed graft survival without evidence of significant rejection, as well as appropriate differentiation of the grafted tissues, but very limited graft–host connectivity and no mass or cyst formation. We recently reported results from autopsies of two long-surviving transplant recipients with HD, and showed graft survival, striatal differentiation, and lack of immune rejection or adoption of HD pathologic changes; however, graft–host connectivity was again very limited [9]. We now report autopsy results from a fourth HD patient with neural transplants, in which, unlike the prior autopsies, we find evidence of graft overgrowth in association with autologous sural nerve co-graft and prominent ependymal cyst formation.

Materials and methods

Patient selection into clinical trial

The neural transplantation and clinical protocols were approved by the Institutional Review Board at Good Samaritan Hospital in Los Angeles, CA, and patients were enrolled only after appropriate informed, written consent was obtained. Patients with pathologic CAG trinucleotide repeat expansion in exon 1 of the Huntington gene were selected based on criteria proposed in the Core Assessment Program for Intracerebral Transplantation for HD [20]. Inclusion and exclusion criteria are detailed elsewhere [10], but included chorea as the primary clinical symptom, radiographically confirmed striatal atrophy, family history of HD, PET scan-confirmed striatal hypometabolism, and no serious complicating medical or psychiatric conditions. Patients were evaluated neuropsychologically and with the original Unified Huntington's Disease Rating Scale (UHDRS) prior to transplantation and post-operatively for 2 years.

Fetal tissue preparation and transplantation

Donor fetuses were obtained according to recommendations established by the National Institutes of Health and as described in detail previously [10]. In this patient, four fetuses between 20 and 32 mm crown-to-rump length (approximate gestational age 9–10 weeks) were used. Whole ganglionic eminence was carefully dissected, and leptomeninges and ependymal lining carefully removed. The lateral ganglionic eminence (LGE) was separated from

medial ganglionic eminence (MGE) and immediately divided into 0.8–1.0 mm^3 pieces. The dissection was performed under sterile conditions in Hank's Balanced Salt Solution supplemented with 10 μg/ml of Gentamicin and 0.25 g/ml of Fungizone (amphotericin B). The LGE pieces were washed ten times in this solution and stored at 4°C until the time of surgery, when tissue viability of >85% was required in order to proceed.

A detailed description of methods for determination of surgical coordinates and implantation procedures has been previously described [10]. The number of grafts and transplant coordinates were determined immediately prior to surgery using brain MRI imaging (GammaPlan software, Version 2.01, Electa, Sweden). In the patient described here, bilateral craniotomies were performed, and a single piece of fetal tissue (80–120 μl) was stereotactically injected at the appropriate coordinates with concomitant retraction of the cannula. At the most posterior right putaminal implantation site, a small length of the patient's sural nerve was deposited along with a fetal graft. Cyclosporine immunosuppression was instituted pre-operatively at a dose of 15 mg/kg and maintained 12 months after the surgery with routine renal function testing.

Gross examination and graft identification

Post-mortem examination was performed after informed written consent was obtained from the patient's legal next of kin according to the patient's wishes and according to protocols approved by the Institutional Review Board of the University of Washington. After immersion fixation in formalin for approximately 4 weeks, the cerebrum was coronally sectioned into approximately 0.5 cm slices while the brainstem and cerebellum were sectioned axially. Representative sections of many brain regions were evaluated while the neostriatum was divided into blocks for thorough analysis. Tissue processing and staining was performed exactly as described previously [9].

Immunohistochemistry

IHC was performed according to published protocols using diamino-benzidine tetrachloride as the chromogen substrate [9]. Primary antibodies were purchased from Chemicon (high molecular weight neurofilament N52, 1:600; microtubule associated proteins MAP-1B, 1:1,500 and MAP-2, 1:1,500; synaptophysin, 1:400; ubiquitin, 1:20,000; myelin basic protein (MBP), 1:1,000; acetylcholinesterase, 1:250), Dako [glial fibrillary acidic protein (GFAP), 1:500; low + high molecular weight neurofilament 2F11, 1:1,700; calretinin, 1:10; CD20, 1:300; CD68, 1:4,000; S100, 1:9,000; and Ki-67, 1:125], Sigma (calbindin-D28K, 1:1,500; parvalbumin, 1:1,500), and Novacastra (CD3, 1:200).

Electron microscopy

Portions of host putamen, graft, and graft-associated peripheral nerve were processed for ultrastructural analysis by fixation in 3% glutaraldehyde, and post-fixation in 1% osmium tetroxide. After polymerization, 1-μm thick sections were cut and stained with Richardson's stain (methylene blue, sodium borate, azure II) for preview. Ultra thin sections (0.1 μm) were cut on selected blocks (Reichert-Jung Ultracut E) and stained with uranyl acetate and lead citrate. Sections were examined using a Philips Electron Microscope (EM410) with high resolution digital camera (AMT XR-400).

Fluorescence in situ hybridization and immunofluorescence

Sections were deparaffinized and then denatured in formic acid/H_2O_2 followed by pretreatment with citrate buffer at 80°C. Protein was digested with pepsin followed by incubation with SpectrumGreen-labeled-X/SpectrumOrange-labeled-Y chromosome probes (Abbott Molecular) in hybridization buffer and Denhyb-2 (Insitus Biotechnologies) overnight. Immunofluorescence was performed on some of the hybridized sections with primary antibodies to GFAP (1:500), S100 (1:900), and MAP2 (1:50), followed by incubation with appropriate secondary antibodies (1:400) conjugated with Cy5 (Jackson ImmunoResearch). All sections were coverslipped with Fluorguard containing DAPI nuclear counterstain (Insitus Biotechnologies).

Results

Clinical history

The subject's father died of HD at the age of 50 and her brother had HD. She initially became symptomatic at the age of 27, when she noticed increased clumsiness and difficulty navigating hills and stairs, mild confusion, computational difficulties, and depression. Genetic testing revealed 48 CAG repeats in the HD gene locus. At the age of 29, while still relatively high-functioning, she received ten fetal neural transplants: four per putamen and one per caudate nucleus, bilaterally. In addition, in order to assess the potential neurotrophic benefits of peripheral nerve and nerve sheath, an autologous sural nerve graft was implanted into the most posterior graft site of the putamen. Her postoperative course was uncomplicated, and clinical follow-up was performed at 3, 6, 9, 12, 18, and 24 months post transplantation.

The patient felt positive about her surgery and insisted that she benefited from the procedure, particularly with respect to memory, attention, concentration, and mood.

Results of proscribed clinical assessments, including UHDRS rating scales during the 2 years of structured clinical follow-up showed stabilization and improvement in some indices, although a subset of these were beginning to worsen at her final clinical assessment (2 years post transplant; see Table 1). After the conclusion of the study in 1998, the patient was followed by her primary neurologist, who in 2001 noted bilateral upper motor neuron and dystonic features, worse on the right, prompting an MRI in 2003 that showed a 3.1 cm cyst in the left putamen and a similarly sized nodular mass in the right putamen (Fig. 1). No signs of increased intracranial pressure were reported. The patient's upper motor neuron symptoms seemed to progressively worsen, but became increasingly difficult to distinguish from coincident HD progression. By 6 years post transplant the patient exhibited choreiform movements of head, face, tongue, and feet; increased posturing and dystonia of head, face, and right leg; and worsening depression, agitation, paranoia, and two possible suicide attempts that prompted transition to skilled nursing care 7 years post transplant. By 9 years post transplant she exhibited coarse choreiform movements, severe dysarthria, incoordination, hyperreflexia, painful extensor spasms, repetitive and sometimes violent behaviors, progressive agitation, hallucinations, and possible seizures. She died 121 months post transplant from complications of advanced HD.

Autopsy findings

The dura had four single sutures overlying the frontal lobes bilaterally. There was no evidence for chronic subdural hematoma. The brain weighed 985 g and showed mild frontal cortical atrophy. Seven cannula tracts (3 on the left, 4 on the right) in the middle frontal gyri were identified without evidence of hemorrhage. Coronal sections revealed multiple lesions (Fig. 1; Table 2). Three mass lesions and one large cyst were present in the left caudate and putamen, with marked mass effect on the internal capsule. Five mass lesions and two cysts (one inside a mass) were identified in the right caudate nucleus and putamen, also with prominent mass effect on the posterior limb of the internal capsule. The mass lesions bilaterally were well-circumscribed and surrounded by scant amounts of firm neostriatal tissue and white matter. Although marked atrophy of the host caudate nuclei corresponded to grade IV HD grossly [25], the lateral ventricles were not enlarged. There was slight right to left midline shift (Fig. 1).

Microscopic and ultrastructural examination

Histologic examination showed intense gliosis of bilateral caudate nuclei and putamen, corresponding to microscopic grade IV HD [25]. Examination of the lesions revealed

Table 1 Clinical and UHDRS assessments

Assessment	Pre-op	+3 months	+6 months	+9 months	+12 months	+18 months	+24 months
Walk 20 feet (s)	20	18	9	10	12	12	11
Read paragraph (s)	21	14	14	15	14	16	18
Recite months backward (s)	23	16	18	14	19	20	23
UHDRS motor (6–20)[a,c]	32	10	11	14	9	10	12
UHDRS behavior (30–35)[a,d]	21	2	0	1	0	2	1
Functional assessment (49–73)[a,e]	26	25	26	30	25	28	28
Functional capacity (75–79)[b,f]	8	11	10	9	8	8	10
Recall three objects after 5 min	2				3		3
Recall seven digit number backward	2				7		6

[a] United Huntington's disease rating scale: included items in (); scores increase with deficit

[b] United Huntington's disease rating scale: included items in (); scores decrease with deficit

[c] Max score 124

[d] Max score 48

[e] Score range 24–48

[f] Score range 0–13

Fig. 1 Radiographic imaging and brain sectioning reveal large left putaminal cyst and multiple masses. **a** Axial T2-weighted MRI in 2003 shows a large cyst in the left putamen (*right side* of image, *black asterisk*) and a large, circumscribed mass in the right putamen (*left side* of image, *white asterisk*). **b** Coronal brain section at the level of the anterior commissure shows four mass lesions (*black arrows*), including a large mass in the left putamen, a smaller mass in the right putamen, and mass occupying the left caudate nucleus, and a cyst encased by a mass lesion in the right caudate nucleus. **c** Coronal brain section at the level of the optic chiasm demonstrating the large left putaminal cyst (*black asterisk*) with prominent mass effect on surrounding structures, including internal capsule, as well as the large right putaminal mass (*white asterisk*). **d** Higher power photograph of anterior left neostriatum seen in **b**. **e** Higher power photograph of right neostriatal mass seen in **c**. **f** Higher magnification image of large left neostriatal cyst wall. *Scale bar* in **b** and **c** indicates centimeters
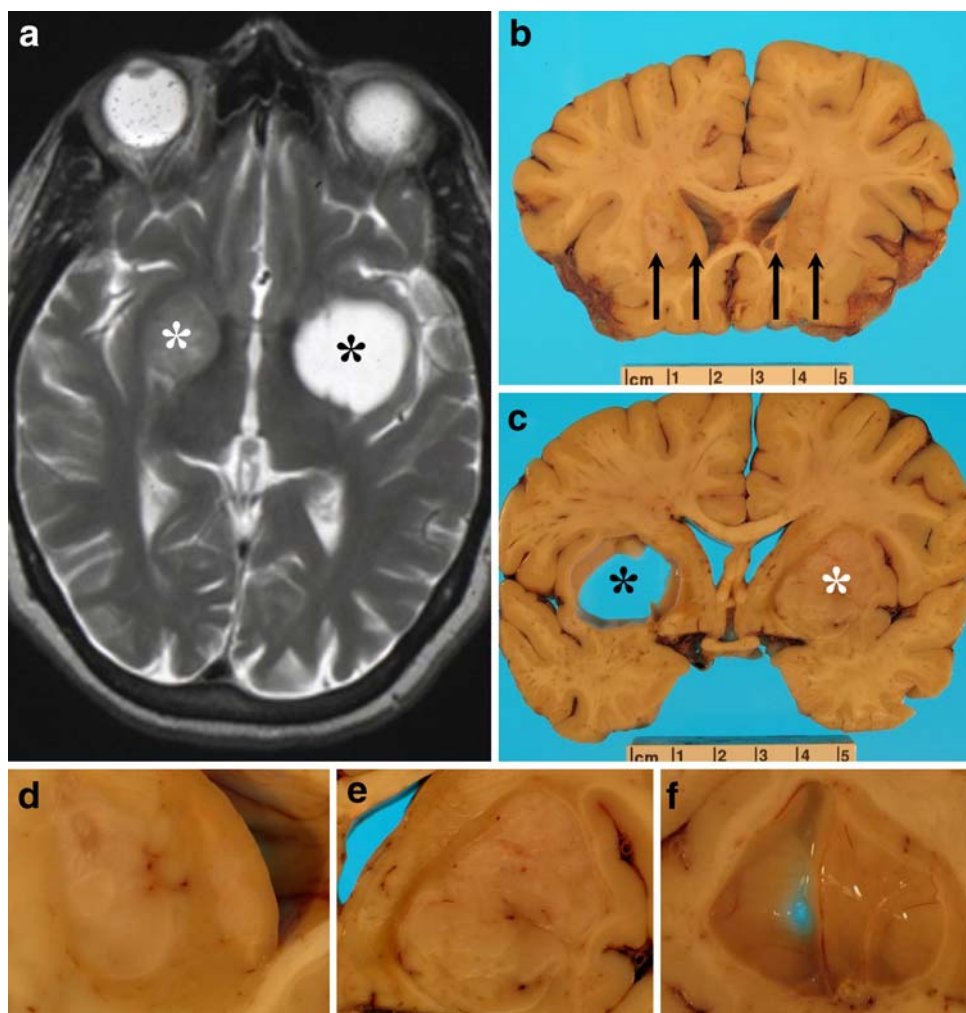
Table 2 Lesion site and karyotype

Site	Lesion	Size (cm)	Karyotype
Right putamen	Mass	2.9 × 1.8 × 1.9	XY
	Mass	1.1 × 1.0 × 0.8	XX
	Mass	1.2 × 0.3 × 0.6	XX
	Cyst	0.7 × 0.3 × 0.3	XY
Right caudate	Mass	0.9 × 0.4 × 0.5	XX
	Cyst	0.3 × 0.3 × 0.2	XX
	Mass	0.4 × 0.4 × 0.4	XX
Left putamen	Mass	0.7 × 0.5 × 0.5	XX
	Cyst	2.0 × 1.9 × 1.5	XX
Left caudate	Mass	1.4 × 0.8 × 1.0	XX
	Mass	1.2 × 0.4 × 0.6	XX

circumscribed masses composed of unorganized neuropil with scattered microcalcifications (Fig. 2) and a diffuse, biphasic population of mostly small and some large neurons interspersed with islands of reactive astrocytes and scattered oligodendrocytes (Fig. 3). The masses contained individual and bundled myelinated axons that rarely appeared to cross the graft–host boundary. The grafts were densely immunopositive for synaptophysin (data not shown) and microtubule-associated protein-2 (MAP-2), and focally positive for MBP (Fig. 2). In addition, graft neurons were uniformly MAP-2 positive, and variably immunoreactive for MAP1B and neurofilaments N52 (high molecular weight) and 2F11 (low/high molecular weight). Calretinin neurons were abundant, and sometimes occurred in clusters, while calbindin- and parvalbumin-positive cells were rare. Neither axons nor dendrites convincingly crossed between host parenchyma and graft tissue, although GFAP immunostaining showed only patchy transplant border gliosis (Fig. 3). Tyrosine hydroxylase (TH) immunopositive fibers were present, but rare, within the graft tissue, and no definitive crossover of TH fibers was identified (Fig. 3). Acetylcholinesterase staining was diffuse and weak within the grafts (data not shown); no clear P-zones were identified. Ubiquitinated neuronal intranuclear inclusions were present in surviving host striatal neurons, but none of these lesions were identified in neurons within graft-derived tissues (data not shown). Tissue autolysis prevented reliable assessment of cell proliferation with Ki-67 antibodies, but no mitotic figures, areas of abnormally increased cellular density, or necrosis was identified in any of the grafts.

The autologous sural nerve graft was identified in the host parenchyma adjacent to the largest mass (Fig. 2), and was characterized by dense collagen and N52- and 2F11-positive unmyelinated axons; no myelinated axons remained in this segment of peripheral nerve. Moreover, while no significant inflammatory infiltrate was identified in any mass lesion, a focally prominent mixed inflammatory infiltrate, composed of CD3, CD20, and CD68 immunoreactive T cells, B cells, and macrophages, respectively, was present in the segment of sural nerve (data not shown). Although in close proximity, no connection between graft or host parenchyma and nerve segment was identified. A small cluster of adipocytes was present within the nerve sheath.

Each cyst was surrounded by piloid gliosis except for the right caudate nucleus lesion, which contained nodular graft neuropil along portions of its wall. The cysts were lined with GFAP-immunopositive, ciliated ependymal cells (Fig. 2).

Ultrastructural analysis was compromised by autolysis. However, prominent glial and neuronal intermediate filaments as well as myelinated axons were identified in graft neuropil (data not shown). The peripheral nerve contained abundant collagen fibers surrounding occasional non-myelinated axons. Host putamen revealed prominent gliosis.

Fluorescence in situ hybridization

All cells in the host parenchyma exhibited an XX karyotype (data not shown). Karyotypic distribution of grafts and cysts is depicted in Table 2 and in Fig. 4. The largest mass lesion in the posterior putamen contained a majority of XY chromosome nuclei (172/200 cells counted). Rare XY cells (2/100 nuclei) could be identified in the host parenchyma immediately adjacent to the graft, but no XY cells were identified greater than a fraction of a mm from the graft in the host parenchyma. XX karyotype cells were present within the male grafts, but were most often endothelial cells or occasional astrocytes (data not shown). Although the largest (left putamen) cyst ependyma was XX karyotype, one of the two smaller cysts (right putamen) was lined by karyotypically male ependyma. The autologous sural nerve graft contained only XX karyotype cells. Co-immunofluorescence labeling in the male graft (Fig. 4) revealed donor-derived oligodendrocytes (S100), astrocytes (S100, GFAP), and neurons (MAP2).

Discussion

We show 10-year survival of karyotypically confirmed transplanted tissue in a patient with HD who showed initial clinical stabilization and, by some indices, improvement. However, we also show, for the first time, the potential for fetal neural transplanted tissue to exhibit overgrowth resulting in mass effect on critical structures of the CNS. Moreover, contamination with karyotypically confirmed fetal ependyma likely resulted in the formation of multiple cysts, contributing to mass effect on the internal capsule with progressive impairment.

Fig. 2 Hematoxylin and Eosin/luxol fast blue staining delineates characteristic features of grafts, peripheral nerve, and cyst wall. ×12.5 Magnification of right (**a**) and left (**b**) putaminal masses. Insets of serial sections stained with MAP-2 (*lower left*) or MBP (*upper right*) show well-demarcated transplant tissue. **c** Autologous sural nerve graft is identified adjacent to the large right putaminal transplant within gliotic host putamen. **d** Higher magnification view of sural nerve graft shows well circumscribed nerve fascicles associated with several adipocytes and focal lymphohistiocytic inflammatory infiltrates. **e** Large left putaminal cyst wall contains patches of intact ependyma, which contain abundant cilia (*inset*, *upper right*) and are GFAP immunopositive (*inset*, *lower left*). **f** Transplanted tissues contain focal microcalcifications (magnified in *inset*). *Tx* transplant, *IC* internal capsule, *PN* peripheral nerve, *MAP-2* microtubule associated protein 2, *MBP* myelin basic protein, *GFAP* glial fibrillary acidic protein
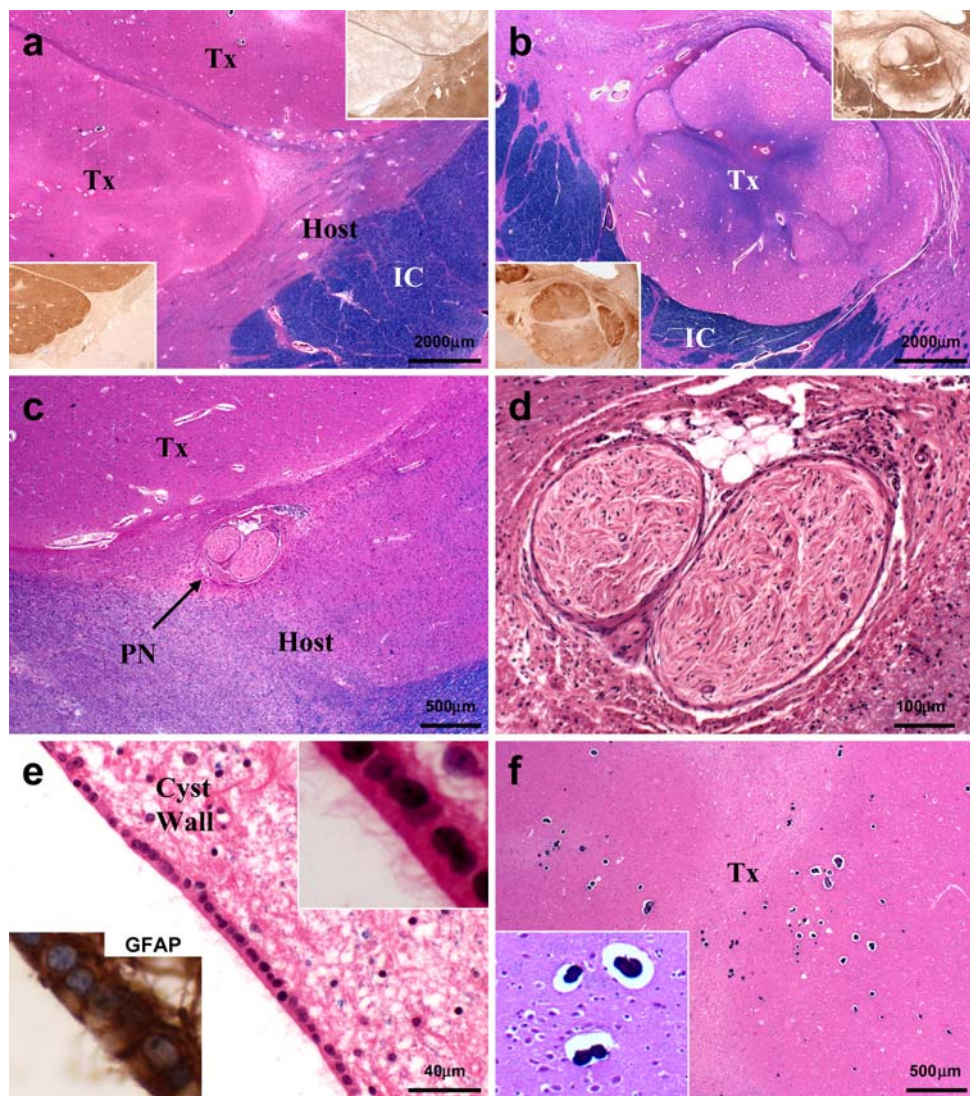
As neural transplantation trials for HD were being designed and initiated, Peschanski et al. [18, 19] discussed transplant overgrowth as a possible complication of neural transplantation in HD. In contrast to other long-term survivors of this procedure who have come to autopsy [9], the singular feature of this case was development of graft-derived mass lesions. Indeed, about 100 μl of tissue was transplanted at each site, but the largest mass occupied roughly 15 ml by the time of death, an approximate 150-fold increase in grafted tissue volume. At the time of surgery, peripheral nerve "co-grafts" for presumed neurotrophic support had shown beneficial effects in host [4] and transplant tissue [26] in a non-human primate model of Parkinson's disease (PD), and at least one clinical trial utilizing autologous peripheral nerve and adrenal medulla "co-grafts" was underway [27]. Interestingly, the largest graft-derived mass in our patient occurred in immediate proximity to the implanted sural nerve segment; however, transplant overgrowth also was observed in other grafts in the ipsilateral and contralateral hemispheres.

Other factors that may have influenced proliferation and graft overgrowth include the relative number of neural stem/progenitor cells initially implanted, graft neuropil formation, angiogenesis, latency from transplant surgery to death, and graft–host sex mismatch. The ganglionic eminence contains abundant germinal matrix, which is composed of dense progenitor cell networks, and utilizing this tissue may be an inherent risk of this procedure. The 10 years' latency in this patient is similar to 6–7 years' latency in the prior autopsies that did not show mass lesions [9], and therefore seems an unlikely explanation for graft overgrowth. The masses were well-vascularized by XX vessels, suggesting angiogenesis from the host, which was likely necessary but not clearly sufficient for transplant proliferation. Finally, since the largest graft was of male origin, the possibility of sex-mismatch overgrowth must be considered; however, this phenomenon has not been reported in other HD transplant patients or in other transplant paradigms. Thus, while many factors may have

Fig. 3 Key microscopic features of transplants and graft–host interaction. *Top half* transplant tissue is shown in the top half of the figure, with H&E/ LFB high magnification center image showing rare mature neurons surrounded by numerous small neurons and occasional glia. *Surrounding pictures*, from *top left* counterclockwise, show immunopositivity of neurons for MAP-2 (uniform), neurofilaments 2F11 and N52 (occasional), calbindin-D28K (rare), and calretinin (common). Graft axons bundles are shown with 2F11 immunostaining, and are further apparent in MBP-stained sections, which also depict occasional haphazard/chaotic tract formation not normally seen in mature brain parenchyma. GFAP immunostains highlight occasional reactive astrocytes present individually or in groups within the masses. *Bottom half* the bottom four photomicrographs show graft–host border with MBP, MAP-2, tyrosine hydroxylase, and GFAP. MBP-immunostains highlight the transverse fiber bundles coursing through host putamen, and graft tissue (outlined in *white*) exhibiting local mass effect without bundled myelinated axons. TH and MAP-2 immunostains further highlight abrupt graft–host border where virtually no neuronal processes appear to cross. GFAP-immunostains show less well-defined border, as local reactive gliosis blurs boundaries, but also highlights general lack of pathology within most grafted tissues
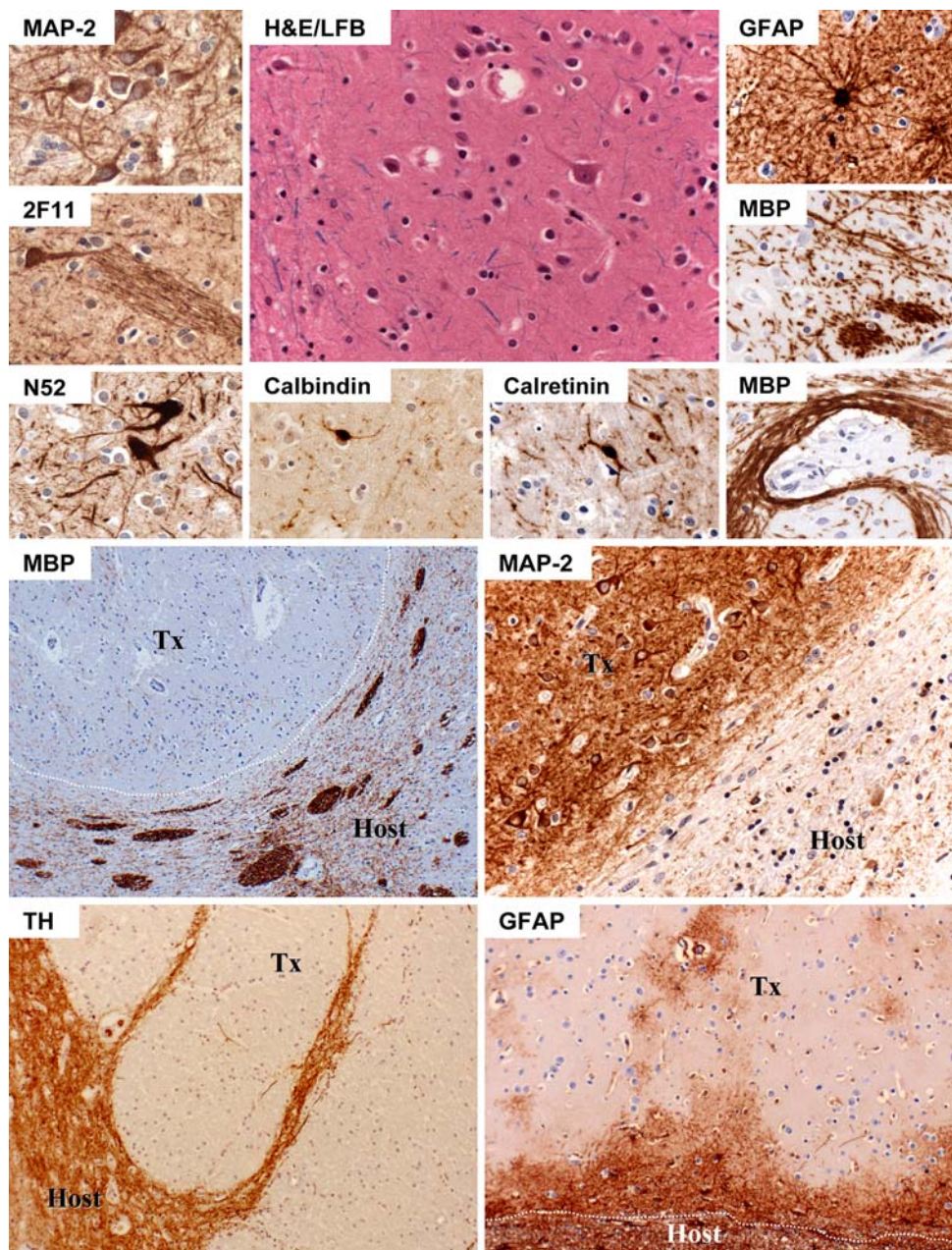
contributed to graft overgrowth, the exact mechanism may never be determined in this case.

In addition to the mass effect from graft overgrowth, significant compression of the left posterior limb of the internal capsule was mediated by an ependymal cyst in the putamen; two other ependymal cysts also were identified within the neostriatum. Ependymal cysts could be host-derived from ependymal rests or ventricular tissues carried by transplant cannulae to the neostriatum, or donor-derived. Although painstaking efforts were made at the time of dissection to remove all ependymal tissues, the adherence of the ependymal cell monolayer makes this virtually impossible in LGE dissection. One of the smaller intrastriatal

ependymal cysts was XY karyotype and therefore donor-derived, but the other two cysts were lined with female cells, making their origin uncertain.

Importantly, although there was slight right-to-left midline shift, clinically the patient's right side was more severely affected, arguing for more significant mass effect from the large ependymal cyst. Compression of surrounding brain by mass lesions was similar bilaterally at autopsy. Since imaging data is only available from 2003, it is unclear when the cystic and solid mass lesions developed in this patient. Although the patient's asymmetric upper motor neuron symptoms were first reported in 2001, symptomatic onset is not known. However, since the relative size of the

Fig. 4 XY chromosome fluorescence in situ hybridization (FISH). Gross (**a**, **b**) and microscopic (**c**–**e**) depictions of graft chromosomal identity, wherein graft masses are labeled with XX for female and XY for male. Cysts are labeled for XX/XY signal in ependyma lining cyst walls (**b**, **c**, **e**). Microscopic sections (**c**–**e**) are stained with antibodies to MAP-2 in order to highlight the grafts. High magnification fluorescence photomicrographs showing astrocytic (**f**), oligodendroglial (**g**), and neuronal (**h**, **i**) differentiation of XY chromosome-positive cells. X chromosomes are stained green and Y chromosomes are stained *red*. Immunostains are colored *pink*, and are labeled accordingly. Note the stellate processes in the GFAP immunopositive astrocyte, variable nuclear immunopositivity in small round nuclei characteristic of oligodendroglia, and the immature (**h**) and mature (**i**) morphology of MAP-2 immunopositive graft neurons
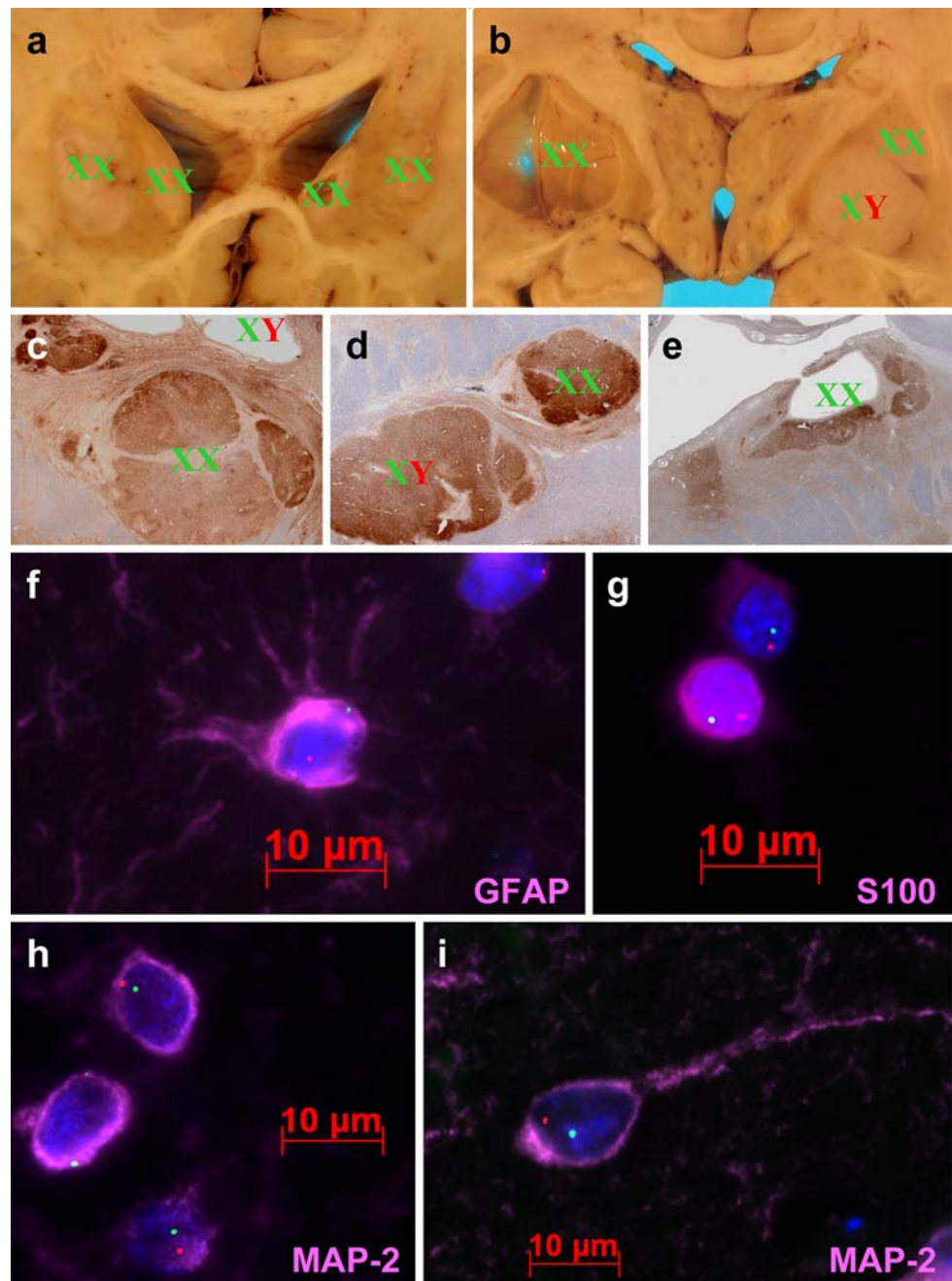
left putaminal cyst and right putaminal graft in 2003 was similar to the size of the same lesions at the time of autopsy, it is likely that the mass lesions were relatively stable between the time of imaging and death.

In support of this, we found no evidence of ongoing cellular proliferation (mitotic activity). Graft overgrowth is not due to the amount of implanted tissue, since a defined volume (0.8–1.0 mm^3) was implanted at each site. Therefore, transient graft cell proliferation waxing from the time of surgery may have resulted in early, robust volumetric expansion, with possible ongoing neuropil production by post-mitotic neurons contributing to overall transplant size.

This was likely influenced by initial graft composition, host factors, and possibly the sural nerve co-graft. Regardless, we interpret graft overgrowth in this case as an excess of "normal" graft tissue, rather than a neoplastic proliferation.

Although graft overgrowth and cyst formation are unique to this case among the three previously reported autopsies of patients with HD who received fetal tissue transplants [7, 9], some features are consistent among these four patients: grafts can differentiate and survive without immunosuppression for many years, few if any neuronal projections cross the graft–host interface, and no HD-type pathologic changes are adopted by graft-derived cells

despite advanced changes of HD in the adjacent host tissue. This latter characteristic is particularly important since, while no neuronal intranuclear inclusions were identified in graft neurons in this case, two of three autopsy studies in long-surviving Parkinson's patients identified Lewy bodies within graft-derived neurons [11, 13, 17]. Consistent lack of neuronal projections crossing the graft–host interface in patients with HD is perplexing since connectivity of transplanted tissue occurs in rodent models of HD and autopsy studies of fetal neural transplants into neostriatum of patients with PD show robust host-graft connectivity [16]. Impaired connectivity repeatedly observed in patients with HD may be intrinsic to transplanted fetal LGE. Another possibility is that reduced connectivity in patients with HD may be related to an unfavorable environment created by the processes of HD. It is interesting to note that graft-derived masses with male karyotype contained blood vessels lined by XX cells, suggesting that, in contrast to neuronal projections, host blood vessels readily transit the graft–host interface.

Two prior reports of pathologic outcomes in neural transplant recipients with PD have been reported [6, 15]; both patients died approximately 2 years post transplant, and both appeared to culminate in ventricular obstruction, hydrocephalus, and herniation. In the Folkerth and Durso report [6], inappropriate fetal elements, noted by Kordower et al. [12] as most likely compromised by "non-CNS structures", were transplanted into caudate nucleus and putamen as well as the lateral ventricle. Mamelak et al. [15] reported a patient who received bilateral putamen transplants resulting in the formation of a large left anterior putamen cyst, which they attribute to inadvertently transplanted fetal choroid plexus; however, Ulrisch et al. [24] refer to additional and unrelated intracranial surgical procedures as possible contributors.

Although only a single case, and despite the lack of connectivity at the time of her death, our patient demonstrated clinical stabilization, and possibly even improvement, in multiple motor, cognitive, and behavioral assessments within 2 years of her surgery. Graft-mediated trophic support of diseased basal ganglia may have contributed, but whether this trophic support continued until her death and was simply overwhelmed by the other pathologic processes, or was transient, cannot be determined. It is important to note that this patient received her transplants early in the course of her disease and at a young age, which may have contributed to her apparent initial improvement.

The results of this investigation are both encouraging and cautionary. The patient's perceived initial clinical improvement made her memorable to those involved in the original trial. It is also encouraging that we can again confirm long-term fetal LGE graft survival and appropriate differentiation without evidence of immune rejection or

adoption of intrinsic pathology, including neuronal intranuclear inclusions. However, consistent lack of evidence for long-term connectivity with host brain raises serious challenges for this approach. Importantly, this case highlights the need to identify those factors that underlie the wide variation in graft (over) growth among transplant recipients.

References

1. Bachoud-Lévi A, Bourdet C, Brugières P, Nguyen JP, Grandmougin T, Haddad B, Jény R, Bartolomeo P, Boissé MF, Barba GD, Degos JD, Ergis AM, Lefaucheur JP, Lisovoski F, Pailhous E, Rémy P, Palfi S, Defer GL, Cesaro P, Hantraye P, Peschanski M (2000) Safety and tolerability assessment of intrastriatal neural allografts in five patients with Huntington's disease. Exp Neurol 161:194–202. doi:10.1006/exnr.1999.7239

2. Bachoud-Lévi AC, Gaura V, Brugières P, Lefaucheur JP, Boissé MF, Maison P, Baudic S, Ribeiro MJ, Bourdet C, Remy P, Cesaro P, Hantraye P, Peschanski M (2006) Effect of fetal neural transplants in patients with Huntington's disease 6 years after surgery: a long-term follow-up study. Lancet Neurol 5:303–309. doi:10.1016/S1474-4422(06)70381-7

3. Bachoud-Lévi AC, Rémy P, Nguyen JP, Brugières P, Lefaucheur JP, Bourdet C, Baudic S, Gaura V, Maison P, Haddad B, Boissé MF, Grandmougin T, Jény R, Bartolomeo P, Dalla Barba G, Degos JD, Lisovoski F, Ergis AM, Pailhous E, Cesaro P, Hantraye P, Peschanski M (2000) Motor and cognitive improvements in patients with Huntington's disease after neural transplantation. Lancet 356:1975–1979. doi:10.1016/S0140-6736(00)03310-9

4. Collier TJ, Elsworth JD, Taylor JR, Sladek JR Jr, Roth RH, Redmond DE Jr (1994) Peripheral nerve-dopamine neuron co-grafts in MPTP-treated monkeys: augmentation of tyrosine hydroxylase-positive fiber staining and dopamine content in host systems. Neuroscience 61:875–879. doi:10.1016/0306-4522(94)90410-3

5. Dunnett SB, Rosser AE (2007) Cell transplantation for Huntington's disease: should we continue? Brain Res Bull 72:132–147. doi:10.1016/j.brainresbull.2006.10.019

6. Folkerth RD, Durso R (1996) Survival and proliferation of non-neural tissues, with obstruction of cerebral ventricles, in a parkinsonian patient treated with fetal allografts. Neurology 46:1219–1225

7. Freeman TB, Cicchetti F, Hauser RA, Deacon TW, Li XJ, Hersch SM, Nauert GM, Sanberg PR, Kordower JH, Saporta S, Isacson O (2000) Transplanted fetal striatum in Huntington's disease: phenotypic development and lack of pathology. Proc Natl Acad Sci USA 97:13877–13882. doi:10.1073/pnas.97.25.13877

8. Hauser RA, Furtado S, Cimino CR, Delgado H, Eichler S, Schwartz S, Scott D, Nauert GM, Soety E, Sossi V, Holt DA, Sanberg PR, Stoessl AJ, Freeman TB (2002) Bilateral human fetal striatal transplantation in Huntington's disease. Neurology 58:687–695

9. Keene CD, Sonnen JA, Swanson PD, Kopyov O, Leverenz JB, Bird TD, Montine TJ (2007) Neural transplantation in Huntington's

disease: long-term grafts in two patients. Neurology 68:2093–2098. doi:10.1212/01.wnl.0000264504.14301.f5

10. Kopyov OV, Jacques S, Lieberman A, Duma CM, Eagle KS (1998) Safety of intrastriatal neurotransplantation for Huntington's disease patients. Exp Neurol 149:97–108. doi:10.1006/exnr.1997.6685

11. Kordower JH, Chu Y, Hauser RA, Freeman TB, Olanow CW (2008) Lewy body-like pathology in long-term embryonic nigral transplants in Parkinson's disease. Nat Med 14:504–506. doi:10.1038/nm1747

12. Kordower JH, Freeman TB, Bakay RA, Goetz CG, Olanow CW (1997) Treatment with fetal allografts. Neurology 48:1737–1738

13. Li JY, Englund E, Holton JL, Soulet D, Hagell P, Lees AJ, Lashley T, Quinn NP, Rehncrona S, Bjorklund A, Widner H, Revesz T, Lindvall O, Brundin P (2008) Lewy bodies in grafted neurons in subjects with Parkinson's disease suggest host-to-graft disease progression. Nat Med 14:501–503. doi:10.1038/nm1746

14. Madrazo I, Franco-Bourland RE, Castrejon H, Cuevas C, Ostrosky-Solis F (1995) Fetal striatal homotransplantation for Huntington's disease: first two case reports. Neurol Res 17:312–315

15. Mamelak AN, Eggerding FA, Oh DS, Wilson E, Davis RL, Spitzer R, Hay JA, Caton WL 3rd (1998) Fatal cyst formation after fetal mesencephalic allograft transplant for Parkinson's disease. J Neurosurg 89:592–598

16. Mendez I, Sanchez-Pernaute R, Cooper O, Viñuela A, Ferrari D, Björklund L, Dagher A, Isacson O (2005) Cell type analysis of functional fetal dopamine cell suspension transplants in the striatum and substantia nigra of patients with Parkinson's disease. Brain 128:1498–1510. doi:10.1093/brain/awh510

17. Mendez I, Vinuela A, Astradsson A, Mukhida K, Hallett P, Robertson H, Tierney T, Holness R, Dagher A, Trojanowski JQ, Isacson O (2008) Dopamine neurons implanted into people with Parkinson's disease survive without pathology for 14 years. Nat Med 14:507–509. doi:10.1038/nm1752

18. Peschanski M, Cesaro P, Hantraye P (1995) Rationale for intrastriatal grafting of striatal neuroblasts in patients with Huntington's disease. Neuroscience 68:73–285. doi:10.1016/0306-4522(95)00162-C

19. Peschanski M, Cesaro P, Hantraye P (1996) What is needed versus what would be interesting to know before undertaking neural transplantation in patients with Huntington's disease. Neuroscience 71:899–900. doi:10.1016/0306-4522(95)00575-7

20. Quinn N, Brown R, Craufurd D, Goldman S, Hodges J, Kieburtz K, Lindvall O, MacMillan J, Roos R (1996) Core assessment program for intracerebral transplantation in Huntington's disease (CAPIT-HD). Mov Disord 11:143–150. doi:10.1002/mds.870110202

21. Ross BD, Hoang TO, Blüml S, Dubowitz D, Kopyov OV, Jacques DB, Lin A, Seymour K, Tan J (1999) In vivo magnetic resonance spectroscopy of human fetal neural transplants. NMR Biomed 12:221–236. doi:10.1002/(SICI)1099-1492(199906)12:4<221::AID-NBM582>3.0.CO;2-Q

22. Rosser AE, Barker RA, Harrower T, Watts C, Farrington M, Ho AK, Burnstein RM, Menon DK, Gillard JH, Pickard J, Dunnett SB, NEST-UK (2002) Unilateral transplantation of human primary fetal tissue in four patients with Huntington's disease: NEST-UK safety report ISRCTN no 36485475. J Neurol Neurosurg Psychiatry 73:678–685. doi:10.1136/jnnp.73.6.678

23. Sramka M, Rattaj M, Molina H, Vojtassák J, Belan V, Ruzický E (1992) Stereotactic technique and pathophysiological mechanisms of neurotransplantation in Huntington's chorea. Stereotact Funct Neurosurg 58:79–83. doi:10.1159/000098976

24. Ulrisch R, Jacques S, Kopyov O (2000) Neural transplantation. J Neurosurg 93:163–164

25. Vonsattel JP, Myers RH, Stevens TJ, Ferrante RJ, Bird ED, Richardson EP Jr (1985) Neuropathological classification of Huntington's disease. J Neuropathol Exp Neurol 44:559–577. doi:10.1097/00005072-198511000-00003

26. Watts RL, Mandir AS, Bakay RA (1995) Intrastriatal cografts of autologous adrenal medulla and sural nerve in MPTP-induced parkinsonian macaques: behavioral and anatomical assessment. Cell Transplant 4:27–38. doi:10.1016/0963-6897(95)92155-R

27. Watts RL, Subramanian T, Freeman A, Goetz CG, Penn RD, Stebbins GT, Kordower JH, Bakay RA (1997) Effect of stereotaxic intrastriatal cografts of autologous adrenal medulla and peripheral nerve in Parkinson's disease: two-year follow-up study. Exp Neurol 147:510–517. doi:10.1006/exnr.1997.6626